T. V. Ramachandra*, Bharath Setturu and Vinayaka Bhatta

Landscape ecological modeling to identify ecologically significant regions in Tumkur district, Karnataka

Abstract: Temporal land use and land cover (LULC) information of a landscape provide an overview of the drivers of change, and impacts on the socio-ecological system. This necessitates organizing diverse data of a landscape, which provides insights into sustainable management. Spatial heterogeneity with landscape dynamics influences biotic and abiotic processes. The knowledge of LULC dynamics aids in assessing the feedback between socio-ecological systems across the urban and rural environments. Visualizing likely landscape changes through modeling help in the decision-making for sustainable landscape management. The current chapter accounts for changes in LULC patterns of the agrarian district Tumkur in Karnataka State, considering temporal remote sensing data of three decades, using geospatial techniques and modeling. Land use (LU) analyses indicate an increase in horticulture area from 0.94 (1989) to 1.02% (2019) due to an increase in commercial cropping. An upsurge of built-up cover from 0.02 to 2.11% (1989–2019) with the enhanced socio-economic activities with the industrialization and infrastructure development across the Tumkur to Bangalore highway. Spatial patterns of landscape dynamics assessed through spatial matrices highlight of increase in urbanization with land conversion from agriculture and forest cover in the outskirts of the Tumkur city center. Ecologically significant regions (ESR) were identified at disaggregated levels through aggregate metrics incorporating bio-geo-climatic, social, hydrological, and ecological aspects. The study region is divided into 9 × 9 km grids for computing metrics at disaggregated levels. ESR is delineated based on the composite metric of all variables, depicts 17 grids (11%) under ESR 1, indicating the highest sensitivity, 29% area (46 grids) as ESR 2 (higher sensitivity), 45% (70 grids) as ESR 3 (high sensitivity), and the rest is 15% (24 grids) in ESR 4 (moderate sensitivity). The outcome of the current research would provide critical management approaches required for managing natural resources

***Corresponding author: Dr. T. V. Ramachandra**, Energy & Wetland Research Group, CES TE 15, Centre for Ecological Sciences, New Bioscience Building, Third Floor, E-Wing, [Near D-Gate], Bangalore, Karnataka, India; Centre for Sustainable Technologies (Astra), Bangalore, Karnataka, India; and Centre for infrastructure, Sustainable Transportation and Urban Planning [CiSTUP], Indian Institute of Science, Bangalore 560012, India, E-mail: tvr@iisc.ac.in. https://orcid.org/0000-0001-5528-1565, https://wgbis.ces.iisc.ac.in/energy

Bharath Setturu and Vinayaka Bhatta, Energy & Wetlands Research Group, Center for Ecological Sciences [CES], Bangalore, Karnataka, India

https://doi.org/10.1515/psr-2022-0154

and will be valuable for policy and planning purposes in pursuing Sustainable Development Goals (SDGs) at the regional scale.

Keywords: forest fragmentation; land use land cover (LULC); prediction; spatial matrices ESR.

1 Introduction

A landscape is a mosaic of heterogeneous ecosystem elements with dynamic components of biotic and abiotic features, which governs the landscape's health. Land cover (LC) depicts the natural cover on the earth's surface, whereas land use (LU) indicates anthropogenic usage of the land, and assessment of these variables aid in understanding the landscape and interactions [1]. The rise in anthropogenic activities including enhanced carbon emissions, has been altering the landscape's natural processes, bio-geoclimatic interactions, hydrological regime, and global climatic alterations [2–6]. The unconstrained land use land cover (LULC) changes induce various ecological imbalances such as fragmentation, loss of resource availability, and interrupted environmental planning. Fragmentation is a devastating ecosystem degradation phenomenon and a conservation challenge that affects habitat integrity induced due to LULC changes in the form of various development projects, the creation of linear corridors, various infrastructure developments, the establishment of industrial parks, and overexploitation resources. Fragmentation of forests contributes to discontinued forest patches of varying sizes, boost biodiversity loss and connectivity, enhances the forest communities' vulnerability, creates a microclimatic environmental gradient, and stimulates invasive species [7–9]. Assessing LULC changes induced fragmentation helps in addressing habitat isolation and edge effects on the forest patches [10, 11].

LULC estimation at a temporal scale forms a base for researchers, policymakers, and planners to determine natural resource availability, frame suitable policies, and evaluate growth patterns [12]. Estimating LULC change has become a crucial strategy for monitoring environmental alterations to manage natural resources, with sustainable planning [13]. Geoinformatics offer consistent remote sensing (RS) data and essential, powerful GIS tools for determining LULC changes at different spatial scales. Spatial metrics, also popularly known as landscape metrics, are other measures that aid in elucidating the landscape's health, with insights of spatial pattern, connectivity, and the effects of human activities on processes [14–16]. LULC mapping has proved to be a beneficial way to assess, advance the choosing areas for different uses, and facilitate accounting for the leading causes and their environmental costs. However, forecasting probable alterations is crucial with respect to resource bases such as land, forest, and water sources in developing nations. Modeling and geo-visualization have become crucial for landscape management, assessing probable anthropogenic-induced changes [17] and their adverse ecological consequences [18]. Modeling assistance in evaluating various conditions for sustainable development, accounting for appropriate spatial

patterns of future LU, and aid as a decision support system (DSS) for regional planners and decision-makers [19]. It also helps empirically interpret the spatial changes and lends the strategies necessitated for landscape conservation through ecosystem protection. The scientific community has devised numerous models that employ statistical [20] and geospatial approaches to understand the landscape dynamics, drivers, and predict likely LU [21]. Well-known predictive LU models are logistic regression models [22], spatial-dynamic model [23], statistical concept-based models CLUE-S [24], hybrid models-Fuzzy, analytical hierarchical process (AHP), stochastic techniques such as spatial Markov chains (MC) [25], cellular automata (CA) [26–28], DYNAMICA-EGO [29], and multi-criteria decision making (MCDM) techniques [17, 19, 30]. The continued increase in LULC changes and per capita resource utilization has resulted in unsustainable landscape exploitation, which signifies the necessity for conservation and the preservation of ecosystem processes for human existence.

Ecologically sensitive regions (ESR) or ecologically fragile zones (EFZ) are diverse distinct regions with distinguishing biotic and abiotic groups, which need to be preserved from further degradation. ESR delineation involves integrating the information of proxy variables of the landscape, such as land, ecology, energy, and social aspects, which stimulates conservation and sustainable management. ESR framework recognizes the significance of ecological, geo-climatic, and social factors available in a region and prioritizes them into distinct units for conservation [31]. In this regard, the objectives of the current research are to (i) examine the spatiotemporal LULC transitions from 1989 to 2019; (ii) assessment of landscape health through forest fragmentation and spatial metrics; (iii) prioritization of ESRs based on their ecological significance; (iv) modeling the likely LU and suggest appropriate policy measures.

2 Materials and methods

2.1 Study area

Tumkur district covers a 10,597 sq. km area, and is located at 12° 45′ to 14° 22′ N 76° 24′ to 77° 30′ E (Figure 1). Chikkamagaluru district surrounds the Tumkur district on the northeast side, Chitradurga and Hassan districts in the west, Mandya district on the south, and Anantapur district of Andhra Pradesh state in the southeast. The district has been divided into 10 taluks: Tumkur, Madhugiri, Pavagada, Koratagere, Sira, Tiptur, Gubbi, Turuvekere Kunigal and Chikkanayakanahalli for efficient administration. The district has a population of 28,82,849 (2021), with a growth rate of 0.9% and has a density of 273 persons/km^2. The gross district domestic product (GDDP) accounts for 57,145 crores (571.45 billion rupees), contributing 3.9% of Karnataka state's Net State Domestic Product. Tumkur city (capital of the Tumkur district) infrastructure has been upgraded under the smart city mission in Karnataka.

The districts have an agricultural-friendly geomorphological and soil composition. Tumkur is covered by denudational uplands on gneisses and granites most of the area.

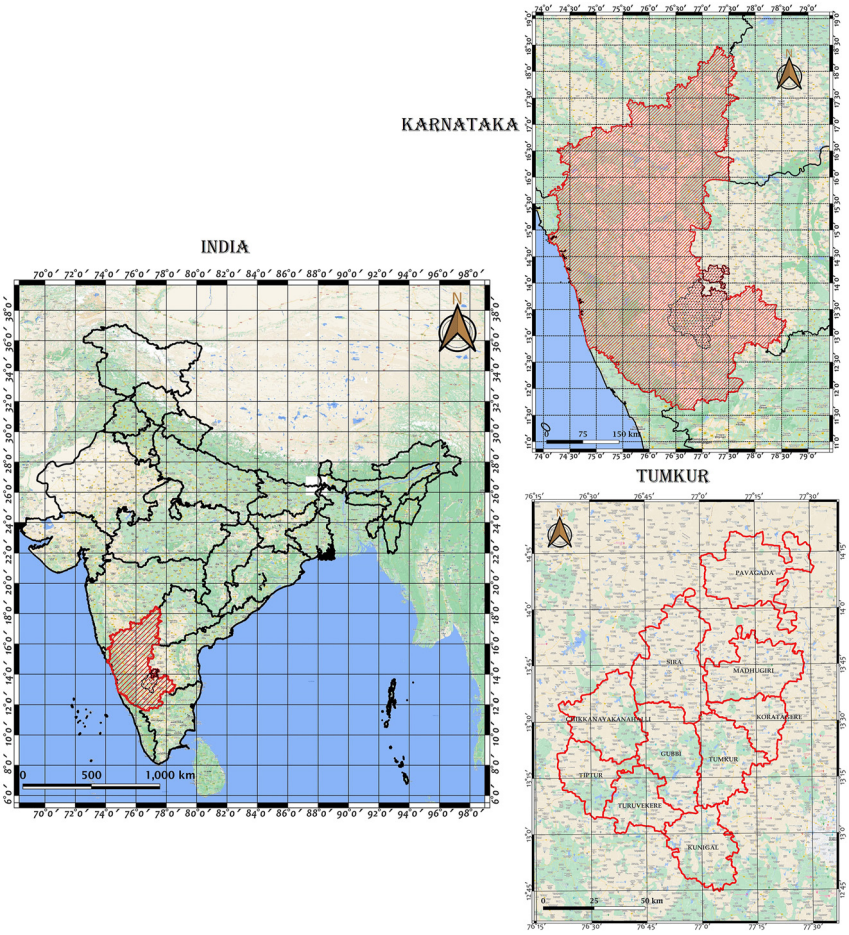

Figure 1: Study area, Tumkur district.

The region receives an average rainfall of 780 mm. The important irrigated crops are paddy, jowar, bajra, maize, ragi, wheat, etc. Major horticultural crops are coconut, ground nut, sunflower, safflower, and castor. Major rivers draining the agriculture fields are Jayamangala, Kumudvathi, Vedavathi, Suvarnamukhi, and Shimsha. None of these rivers are perennial due to catchment degradation with the sustained anthropogenic pressures. Borewells are the primary source for drinking water supply and irrigation. Livestock includes 5,27,067 Cattles, 1,81,118 Buffaloes, 10,61,330 Sheep's, 3,26,890 Goats, 7122 pigs, and 21,07,798 poultry. The tourism sector attracts a large population inflow due to Devarayan Durga temples, Shanishvara temple, Pavagada fort, Siddaganga Mutt, Siddara Betta, Yediyur, Kaggaladu Bird Sanctuary, Marconahalli, etc. The district shelters 37 large scale, 28 medium scale, 309 small scale, 28,452 microscale industries, and 7 industrial estates. Industries such as Hoidel

Berg Cement India Ltd., Turuvekere, HMT Watch Factory Ltd, Tumkur Mann & Hummen Filter Pvt Ltd. Support livelihood for thousands of people. The world's third-largest solar park (photovoltaic) is situated in the Pavagada region, covering 13,000 acres of the district with a capacity of 2050 MW.

2.2 Methods

2.2.1 Quantification of landscape dynamics and assessing spatial configuration through metrics

The primary data (RS data of 30 m spatial resolution) is collected from Landsat archives available in public domains from 1989 to 2019. Pre-processing of RS data has been done to maintain geometrical and radiometric consistency. The secondary data used in the analysis includes the survey of India (SoI) toposheets of 1:50,000 and 1:2,50,000 scales, administrative reports, and virtual earth data sets (BHUVAN; Openlayers; Google Earth). The training data has been collected from the field using a hand-held global position system (GPS) instrument covering distinct landscape features across the district. LC change has been evaluated through NDVI measure, which provided area coverage under vegetation, and non-vegetation based on spectral reflectance property. The range of NDVI for a given pixel is –1 to +1 as per Eq. (1). LU analysis has been carried out using supervised classification techniques such as Gaussian maximum likelihood classifier (GMLC), which accounts for the probability and cost functions, proved efficient compared to other algorithms. 60% of the training data collected from the field has been used for RS data classification, rest of the 40% was used for the accuracy assessment. The classification accuracy (overall accuracy (OA), producer accuracy (PA), user accuracy (UA)) was estimated using reference data by assessing Kappa statistics and overall accuracy.

$$\mathrm{NDVI} = (\mathrm{NIR} - R)/(\mathrm{NIR} + R) \tag{1}$$

Landscape's status has been valued through fragmentation analysis and spatial metrics. The spatial/landscape metrics were calculated at the grid level to assess the landscape configuration [32] through the software Fragstat. The details of the metrics calculated are presented in Table 1. Temporal LU data has aided in assessing fragmentation under various categories based on P_f and P_{ff} indicators by using a 5 × 5 kernel as depicted in Eqs. (2) and (3) [33]. The categories include "Interior forest ($P_f = 1$; i.e., all pixels in the neighboring area are forest); edge forest ($P_f > 0.6$ and $P_f – P_{ff} < 0$; i.e., the majority of the pixels in the neighbouring area are forest but pixels were appearing along the boundary of the non-forest categories such as built-up area, or agriculture), perforated forest ($P_f > 0.6$ and $P_f – P_{ff} > 0$; most of the pixels in the surrounding area were forested, but they appear to be part of the inside edge of a forest patch, or a small clearing was done inside a patch), patch forest ($P_f < 0.4$; i.e., only few forest pixels were present as an isolated segment on a

Table 1: Spatial metrics assessed.

Indicator	Formula	Scale	Justification
CA: Class Area	–	>0	Overall LU class area expressed in hectares
NP: Number of Patches	NP = n NP equals the number of patches in the landscape	NP > 0, without limit	It signifies fragmentation property based on the number of patches accounted in a landscape. The higher the value, the greater the fragmentation and vice versa
AI: Aggregation Index	$AI = \left[\sum_{i=1}^{m}\left(\frac{LA_{ii}}{\max \rightarrow LA_{ii}}\right)P_i\right](100)$ LA_{ii} = number of like adjacencies (joins) between pixels of patch type (class) I based on the single count method max-LA_{ii} = maximum number of like adjacencies (joins) between pixels of patch type class i based on single count method P_i = proportion of landscape comprised of patch type (class) i	$1 \leq AI \leq 100$	AI value represents the grid's agglomeration and scattering of patches. AI corresponds to 1 as maximally disaggregated and 100 as maximally aggregated into a single compact patch
NLSI: Normalized Landscape Shape Index	$NLSI = \frac{\sum_{i=1}^{i=N}\frac{p_i}{a_i}}{NP}$ where a_i and p_i are the area and perimeter of patch i, and NP is the total number of patches	$0 \leq NLSI < 1$	Shape complexity is bestowed with the NLSI index. Increases for greater disaggregation and becomes 0 when the landscape consists of compact or a single square patch

non-forest category), transitional forest ($0.4 < P_f < 0.6$; i.e., half of the neighbouring pixels were forest, and they may be found as a part of a patch, edge, or perforation subjected to the spatial pattern of forest sampled)." The study area was divided into $5' \times 5'$ or $9 \times 9\ km^2$ uniform grids comparable to the SOI 1:50,000 scale toposheet divisions.

$$P_f = \text{Number of forest pixels/Total number of non} - \text{water pixels} \quad (2)$$

$$P_{ff} = \text{Number of forest pixel pairs/Number of forest pixel pairs} \quad (3)$$

2.2.2 Modeling of landscape dynamics through hybrid Fuzzy AHP Markov CA

Modeling landscape dynamics is implemented using Fuzzy AHP Markov CA by considering (i) Markov chain (MC) based transitions from earlier LU data, (ii) estimating

the influences of elements responsible for LU transitions and restricted regions for the LU change, (iii) weightage metric score constructed through Fuzzy AHP and site suitability maps creation with MCE, (iv) simulation and future prediction of LU by MC–CA algorithms. Probable LU for the year 2029 is calculated as outlined in Figure 2. Socio-economic factors influencing LU, including proximity to roads, bus stations, city centers, industries, schools, and social amenities, were considered. Constraints considered for LU transition were water bodies, reserved forest, slope, elevation and wildlife sanctuaries.

LU of 1999, and 2009 were utilized for MC analysis to compute the transition probability. MC reveals the transfer rate among the two different LU classes [34, 35]. The transition probability (TP) for a class i and j can be calculated by Eq. (4).

$$\mathrm{TP}_{ij} = \frac{n_{ij}}{n_i} \tag{4}$$

where n_i is the total number of pixels of class i transformed over the transition period, n_{ij} is the number of pixels transformed from class i to j. The distribution of each LU class at time t+1 is derived with the help of M_t i.e., LU distribution at the beginning time t as (Eq. (5))..,

$$M_{t+1=}\ \mathrm{TP}\star M_t \tag{5}$$

The transition matrix (Eq. (6)) can be shown as

$$M = \begin{matrix} M_{11} & M_{12} \ldots \ldots & M_{1n} \\ \vdots & \vdots & \vdots \\ M_{n1} & M_{n2} & M_{nn} \end{matrix} \tag{6}$$

This calculated transition matrix then used as rate of change to predict the future LU. To find out nth growth rate, let P be the transition matrix of a Markov Chain, and let U be the probability vector that represents the early distribution. Then the

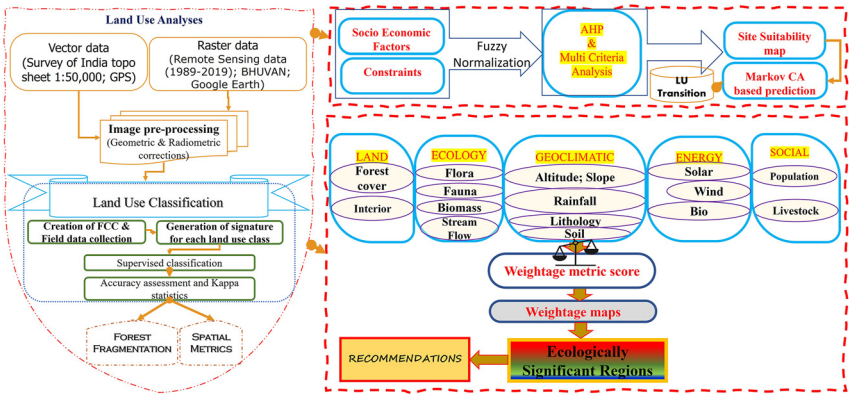

Figure 2: Method utilized for the analyses.

probability that the chain is in the state S_i after n steps is the ith entry in the vector (Eq. (7)).

$$u^{(n)} = uP^n \tag{7}$$

The contributing factors influence on LU transition were accounted by normalizing between 0 and 255 through fuzzification, where 255 indicates the maximum probability of change, while 0 indicates of no changes. AHP has been aided for producing the pair-wise comparison matrices depicting relative weights as Eigenvectors [36] to determine the degree of significance between factors i and j on LU transition. A response matrix $R = [r_{ij}]$ is constructed to quantify the relative dominance of items i over j with the decision maker's assessments, which adhere to a uniform probability distribution (Eq. (8)).

$$r_{ij} = \frac{W_i}{W_j} * e_{ij} \tag{8}$$

where, W_i and W_j are the priority weights belonging to vector W and $\sum W_j = 1$, e_{ij} is inconsistency observed in the analysis. The consistency ratio and consistency index were calculated to estimate the consistency of the judgment matrix by comparing it with random index and maximum eigenvalues. Site suitability map has been generated with the aid of MCE and provided as an input for MCA-based prediction.

2.2.3 Conservation of landscape through ESR prioritization

ESRs were identified at the grid level by applying aggregated weight criteria (Eq. (9)) produced from several themes depicting landscape conditions (i.e., forest cover, forest intactness, biological richness, biomass, social status and energy prospects). The data corresponding to each theme was collected from the field or published literature, published datasets, or administrative reports.

$$\text{Weight} = \sum_{i=1}^{n} W_i Q_i \tag{9}$$

where n is the number of data sets, Q_i is the quantity associated with criterion i, and W_i is the weight associated with that measure. An indicator illustrates each measure represented by a normalized value between 10 and 2. The higher conservation priority was depicted by the value of 10, and the low conservation as 2. The intermediate values such as 8, 6 and 4 correspond to high, moderate and low levels of conservation. The weights were based on a specific factor's quantity assigned across grids. Grids based on the aggregation score were grouped into four groups (ESR 1–4) based on the mean and standard deviation. The groups were formed as ESR 1 (aggregated score > $\mu + 2\sigma$), ESR 2 (for grids within $\mu + 2\sigma$ and $\mu + \sigma$), ESR 3 (for grids with $\mu + \sigma$ and μ) and ESR 4 (grids with values < μ).

3 Results & discussion

3.1 Modeling landscape dynamics and spatial configuration of Tumkur

LC of Tumkur district is assessed by computing NDVI over a temporal scale depicts the area under vegetation and non-vegetation (Figure 3). The vegetation cover has lost from 98.62 (1989) to 95.82% (2019) with an increase in area under non-vegetation (1.38–4.18%).

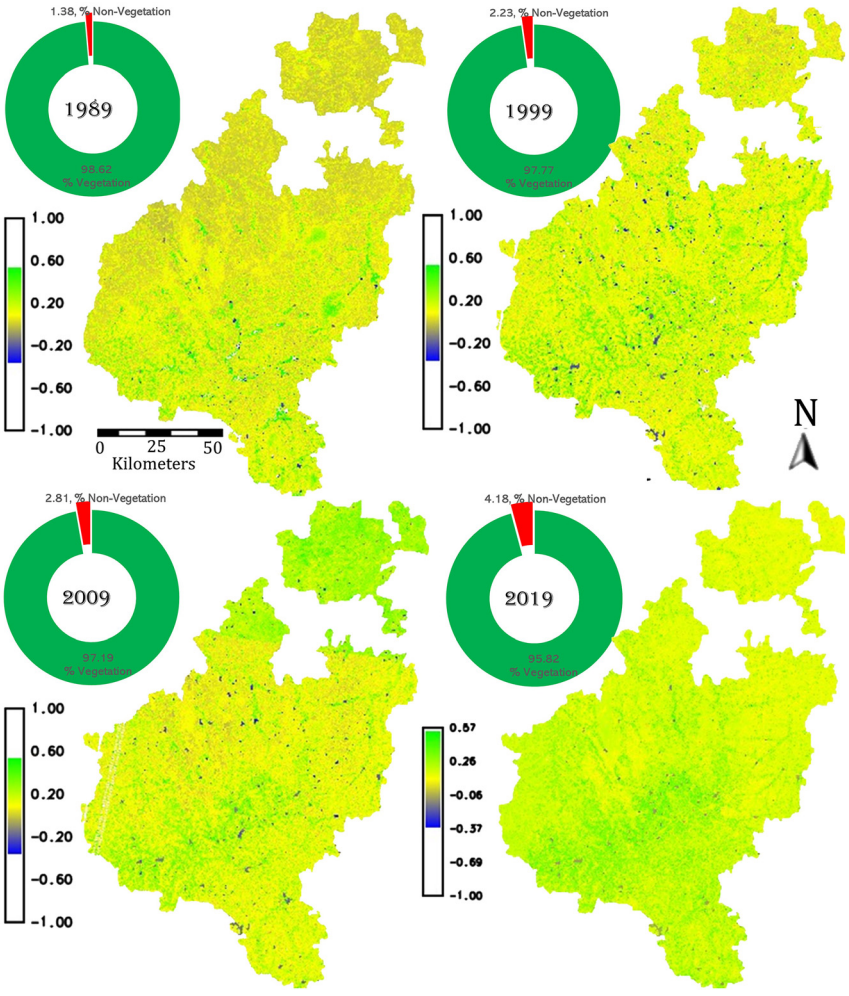

Figure 3: Land cover dynamics in Tumkur.

LU analysis highlights the intense anthropogenic-induced changes post 1999 (Figure 4). The region has lost agriculture and horticulture areas along the national highways (NH), the peri-urban area of Tumkur city, and NH-48. There is a significant increase in built-up cover (0.02–2.11%), and marginal increase in horticulture (0.94–1.02%) and forest plantation (0.13–0.2%). Higher profits in horticultural products and the water availability with the higher number of borewells aided in the increase of horticultural areas along highways. But, post-2000, horticulture areas have been converted into built-up areas due to the expansion of highways. Scrub-land decreased from 21.59 (1989) to 7.29% (2019) (Table 2) with the transition of

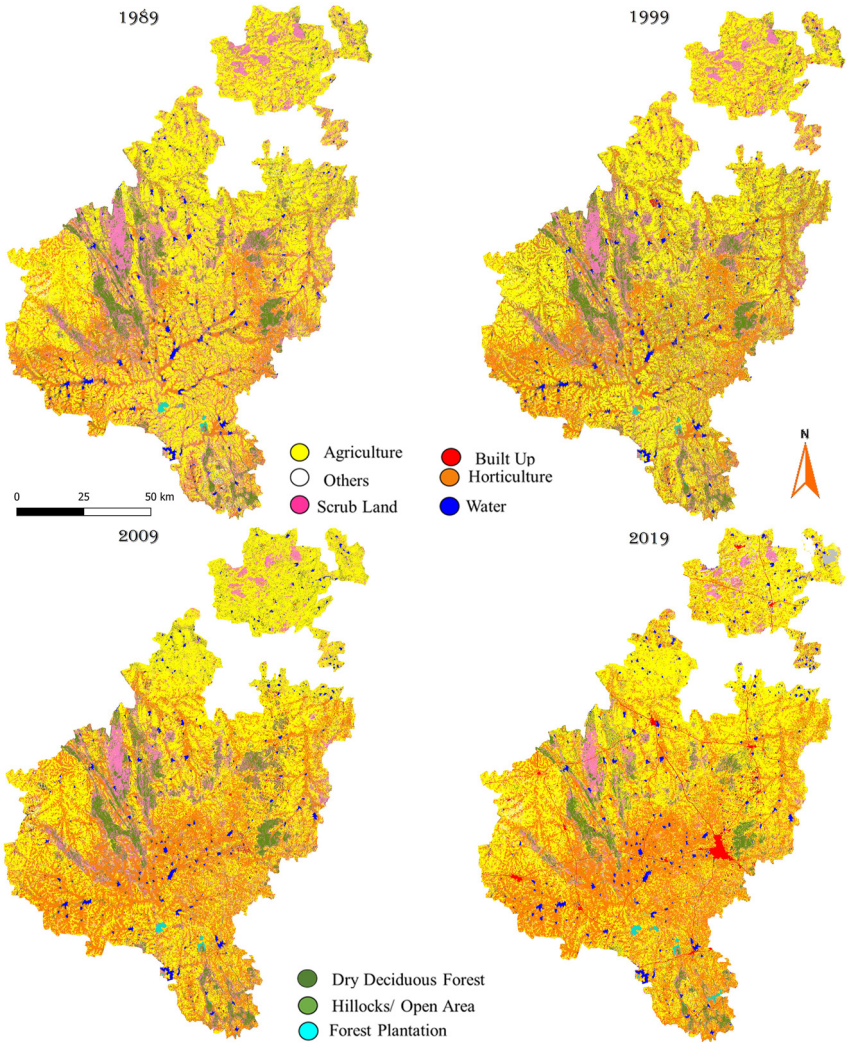

Figure 4: Spatio temporal LU change in Tumkur district.

Table 2: LU dynamics in Tumkur from 1989 to 2019.

Year	1989		1999		2009		2019	
Category	**Sq km**	**%**	**Sq km**	**%**	**Sq km**	**%**	**Sq km**	**%**
Agriculture	5196.80	49.04	4817.3	45.46	4932.74	46.55	5164.92	48.74
Built up	1.78	0.02	59.3	0.56	138.88	1.31	224	2.11
Dry deciduous	1104.8	10.43	869.15	8.20	739.7	6.98	460.08	4.34
Horticulture	99.73	0.94	852.38	8.04	359.4	3.39	108.11	1.02
Hillocks	1635.55	15.43	2097.25	19.79	2856.32	26.95	3492.24	32.95
Others	107.63	1.02	183.37	1.73	109.57	1.03	122.63	1.16
Scrubland	2288.35	21.59	1541.58	14.55	1295.59	12.23	772.7	7.29
Water	148.25	1.40	166.12	1.57	150.71	1.42	192.6	1.82
Forest plantation	14.13	0.13	10.57	0.10	14.11	0.13	21.29	0.20
Solar panels	–	–	–	–	–	–	38.45	0.36

scrubland to horticulture land. Dry deciduous forests decreased from 10.43 (1989) to 4.34% (2019). Solar installation in the Pavagada taluk has resulted in the conversion of barren agriculture areas but aided in meeting electricity demand through renewable sources. Rampant mining also contributed to the forest cover loss and higher instances of human-animal conflicts. The OA and the kappa statistics is presented in Table 3. Field investigation and Google earth data sets were used to analyze accuracies, ranging from 87 to 96%.

LU transition from 1989 to 2019 indicates a greater loss in the dry deciduous class from 1104.80 to 460.08 sq km (Table 4). The increased commercial value of horticulture crops has resulted in large-scale agricultural land conversion into horticulture at Tiptur

Table 3: Accuracy assessment of temporal data.

Year	1989		1999		2009		2019	
Category	**PA**	**UA**	**PA**	**UA**	**PA**	**UA**	**PA**	**UA**
Agriculture	100.0	93.7	99.43	93.60	100.0	79.3	96.93	97.14
Built up	100.0	67.7	6.19	98.90	100.0	54.9	31.34	89.66
Dry deciduous	100.0	62.1	88.16	55.57	78.7	93.9	92.84	100.00
Hillocks	100.0	93.0	96.02	83.70	94.5	67.9	95.86	61.10
Horticulture	100.0	74.0	93.83	91.93	99.0	69.9	95.81	98.57
Scrubland	100.0	74.4	99.65	99.47	100.0	85.9	90.25	54.62
Water	77.7	100.0	94.81	87.53	99.4	79.1	99.44	97.20
Others	100.0	100.0	96.91	46.33	55.6	97.4	60.87	87.51
OA	90.19		89.00		87.0		95.49	
Kappa	0.85		0.84		0.82		0.93	

Table 4: The transition of LU from 1989 to 2019.

		Land use of 2019									
	Category	**Agriculture**	**Built up**	**Dry deciduous**	**Horticulture**	**Hillocks**	**Others**	**Scrubland**	**Water**	**Forest plantation**	**1989**
Land use of 1989	Agriculture	3625.57	99.4	0	47.8	1338.13	59.91	0	25.45	0.56	5172.64
	Built up	0.04	1.73	0	0	0.01	0.01	0	0	0	1.78
	Dry deciduous	322.24	20.5	460.08	13.82	232.48	21.35	0	30.99	3.59	1104.80
	Horticulture	51.29	4.83	0	4.32	34.39	3.08	0	1.79	0.04	99.73
	Hillocks	366.81	40.7	0	6.97	1201.96	8.02	0	10.96	0.12	1635.55
	Others	43.07	8.29	0	1.61	12.89	40.45	0	1.34	0	107.63
	Scrubland	737.68	46.4	0	32.57	639.11	26.53	772.7	29.39	3.97	2288.35
	Water	18.14	2.96	0	1.03	32.24	1.09	0	92.78	0.01	148.25
	Forest plantation	0.08	0	0	0	1.05	0	0	0	13	14.11
	2019	5164.92	224	460.08	108.11	3492.24	160.43	772.7	192.6	21.29	

taluk due to canal irrigation from Vedavathi river. The industrialization, highway expansion, and establishment of an industrial estate at Dabaspet (outskirts of Bangalore city) have increased built-up cover. Rapid industrialization from post-2010 resulted in new satellite towns along the highways. The large-scale agriculture and horticulture lands have been cleared and kept barren for conversion into buildings or industries, which has become a key policy and governance challenges in the district.

Fragmentation analyses emphasize the loss of interior forest cover due to anthropogenic pressures. Temporal fragmentation indicates the changes in urban fringe LU that significantly affect natural resources, especially natural habitat ecosystems, through their impacts on soil and water quality and climatic systems. The analysis reveals the decline of interior forests (10.07–3.68%) due to LU changes (Figure 5). Patch class has decreased from 4.79 to 2.22%, transitional class decreased from 6.38 to 1.95%, edge class decreased from 0.88 to 0.36%, perforated class decreased from 9.38 to 3.51%, interior lost its area from 10.7 to 3.68%. The new patches are created in the interior forest areas due to monoculture plantations and anthropogenic-induced LU features. The loss of interior cover is driving the wild animals to stray into the human habitats in search of food, fodder and water.

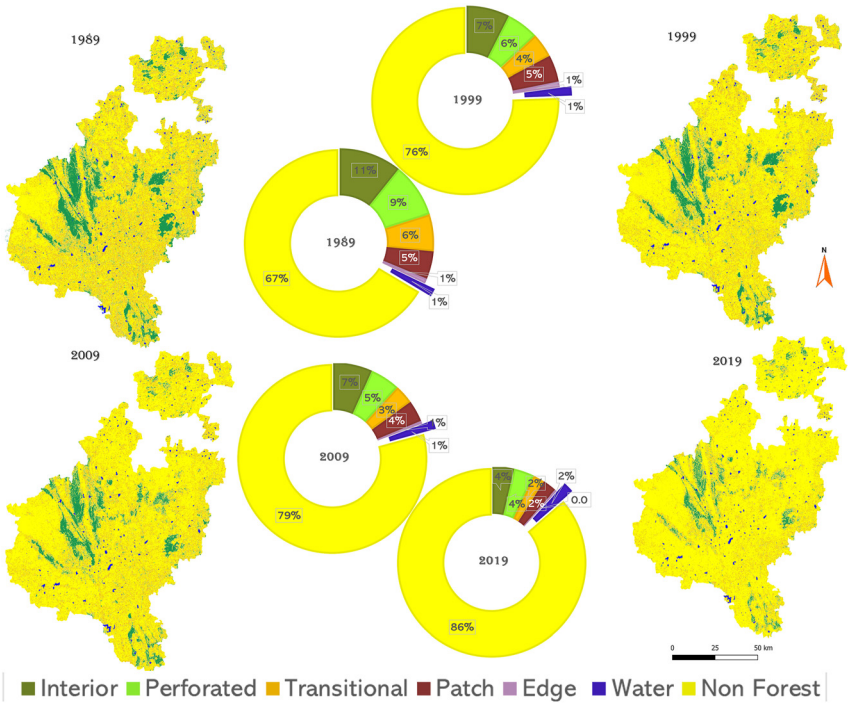

Figure 5: Temporal change in forest structure.

The spatial pattern of built-up and forest categories at decentralized level (9 × 9 km grids) were assessed through the computation of spatial matrices, namely class area (CA), number of patches (NP), normalized landscape shape index (NLSI), aggregation index (AI). CA highlights an increase in the built-up area during 1989–2019 (Figure 6). The main changes were noticed in the grids of taluks Tumkur, Tiptur and Madhugiri. Forest class depicts the loss of CA due to increased fragmentation. NP indicates the extent of fragmentation in landscape with value 0 indicating clustering of patches into a single built-up patch, while higher values indicate the increase in fragmentation. An increase in NP value in the Tumkur, Tiptur and Sira taluks area depicts the urban sprawl or dispersed growth. With the decrease in the forest area, there has been upsurge in number of forest patches with lesser area coverage especially in the Madhugiri region (Figure 7). NLSI shows Tumkur and Tiptur taluks are undergoing intense urbanization with higher spatial complexity (Figure 8). NLSI for forest class shows increased spatial complexity due to urban sprawl and forest cover loss. NLSI values around the city centers increased, indicating the decline of the forest cover. AI value of 100 represents all the patches becoming clusters, while 1 shows the ungrouping of the class. An increase in AI value indicates the compacted growth in cities such as Tumkur, Madhugiri and Tiptur (Figure 9). In contrast, peri-urban region grids show lower values due to new clusters, especially in Tumkur and Tiptur outskirts. Decrease in AI value indicating ungrouping, especially along the Madhugiri, Kunigal and Koratagere taluks.

The distance influence of each factor on LU is evaluated and weighed for projection. The consistency index of 0.04 shows acceptable consistency in AHP index as compared with the standard of 0.1. MCE helped to derive the probable LU transition maps and CA Markov aided in projection of likely land uses based on AHP and MCE

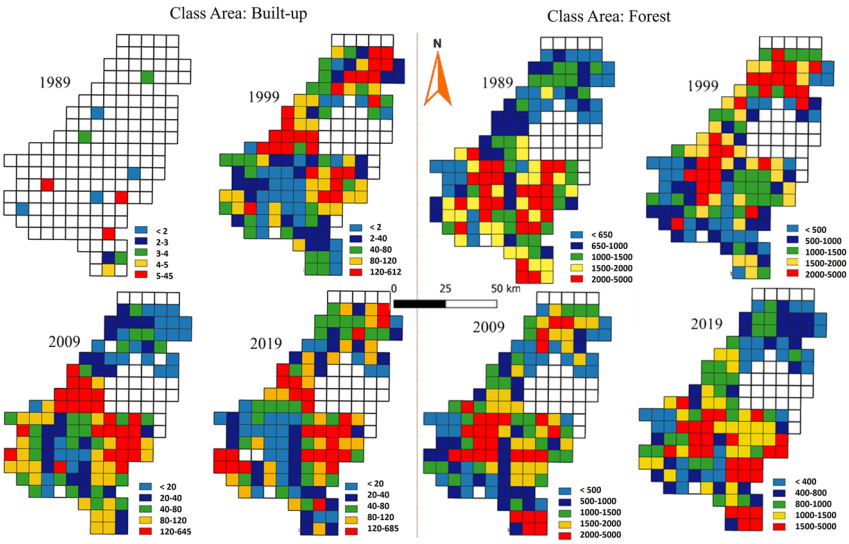

Figure 6: Class area matrix for built-up, forest classes over time.

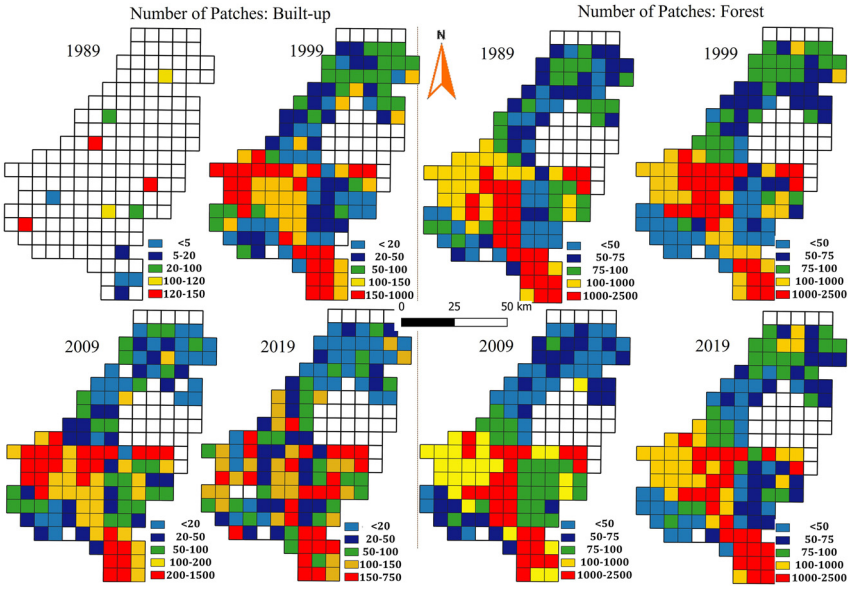

Figure 7: Number of patches of built-up and forest categories.

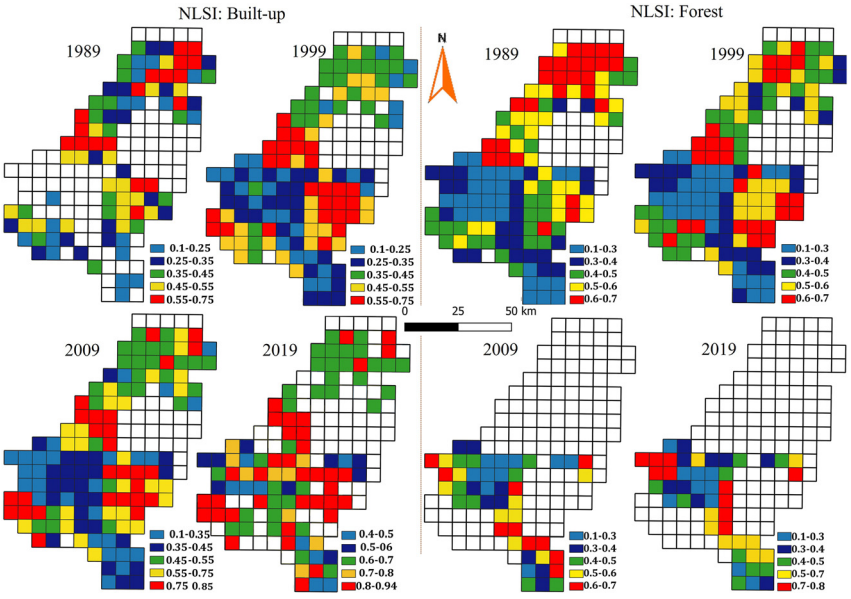

Figure 8: NLSI index of forest and built-up categories.

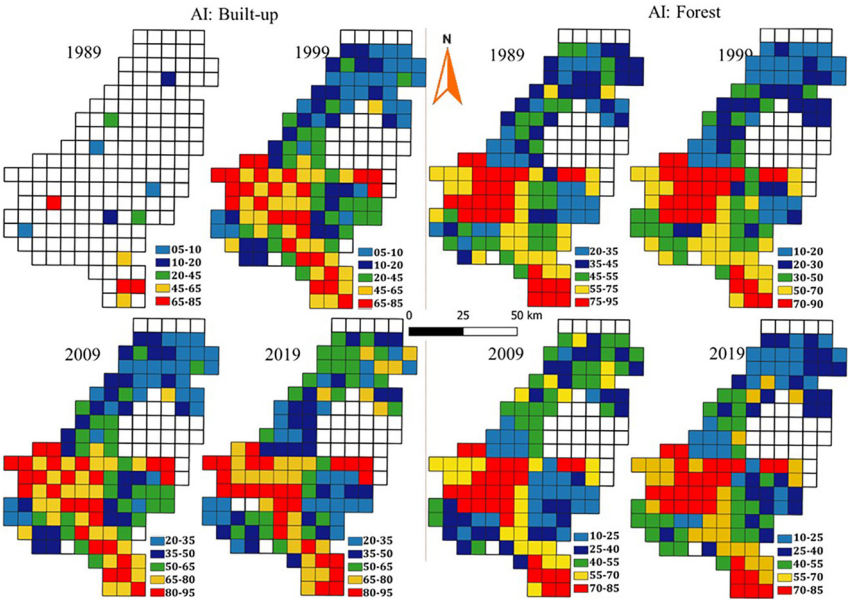

Figure 9: AI index of forest and built-up categories.

inputs. The simulated 2019 map has been compared with actual LU of 2019 and depicted good Kappa value of 0.92 with spatial consistency. The projected LU of 2029 portrays large-scale changes in agriculture with the increase in horticulture and built-up areas. Tumkur city might be expanded further by transforming large tracts of agriculture patches into the Bangalore highway. Intensified horticultural activity influences the transition of forest and agricultural land into monoculture activity, which is the most observed trend in the Tumkur district. Agricultural land decrease from 5164.92 (2019) to 4812.08 km^2 (2029) (Figure 10). Built-up area is likely to increase from 2.11% (224 km^2) to 4.58% (489.11 km^2).

3.2 Prioritization of Ecologically Sensitive Regions (ESRs) for conservation and sustainable development

ESRs at disaggregated levels in the Tumkur district was determined by considering land, geo-climatic, hydrological, energy, social and ecological parameters. The parameters such as biomass, fauna, flora, stream flow, population density, livestock, % forest cover, % interior forest, digital elevation model, perception, % slope, soil type, lithology, bioenergy, wind energy, solar energy etc., have aided in assessing the landscape's capability and significance. The weights were assigned at grid level based on their importance in maintaining the ecosystem and supporting livelihood. Forest cover and the interior forest cover variables imply the health of a landscape. Fragmentation of

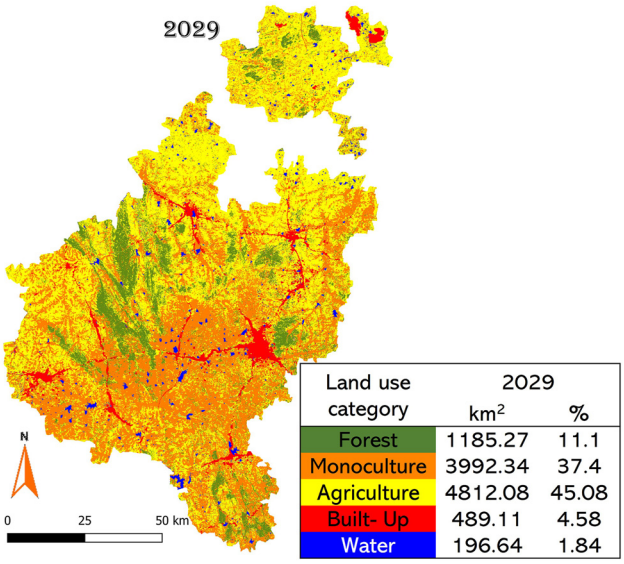

Figure 10: Likely LU of Tumkur.

forests can degrade habitat of species, leading to enhanced human–wild animal conflicts, inbreeding and ultimately the excision of species. Madhugiri, Kunigal and Tiptur regions have major forest and interior forest cover, weights were assigned based on the range (Figure 11).

The energy prospects in the district have been assessed by considering solar, wind and bioenergy potential to understand the district's renewable energy options (Figure 12). The district has uniform solar insolation of >6 kW/h, which helps solar energy harvest at decentralized levels. The wind velocity of the district shows 2.5–4 m/s, emphasizing the capacity for hybrid renewable energy production by integrating solar and wind options to meet the regional energy. The district has uniform bioenergy potential due to moderate bioresources availability.

The ecology in the district has been assessed through various proxy variables, as depicted in Figure 13. Forest cover change with the unrestrained LULC changes can diminish water flow in the streams and rivers, which is detrimental to the biodiversity and livelihoods of people in the district. Stream flow assessment across the grids highlights the region covered by forests has water availability of >6 months, whereas other areas show lower flow. Duration of stream flow is higher in the Tiptur, Kunigal and Chiknayakanhalli regions. Streams in the Vedavathi river catchment with good forest cover house diverse native plant species, confirming the linkage between ecology and hydrology in the catchment. This provides invaluable insight to the need for integrated approaches in river basin management in an era dominated by mismanagement of river

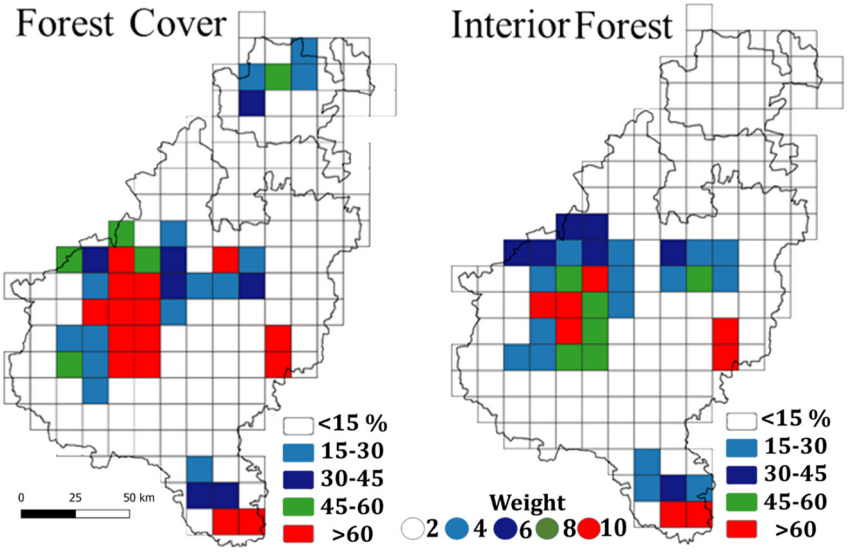

Figure 11: Forest cover and interior forests of Tumkur and weight.

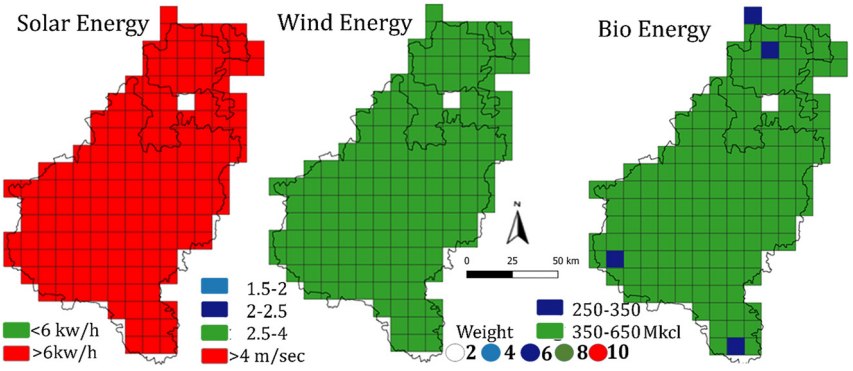

Figure 12: Energy prospects assessed and their weights.

catchment with the enhanced deforestation process, inappropriate cropping, and poor water efficiency [37]. Higher biomass can be seen in Madugiri Forest or Timmalapura Forest, whereas other regions show the least biomass (Figure 13). The spatial distribution of flora and fauna species across the district was compiled through field sampling and literature review. The distribution of the species was assessed as per the IUCN Conservation Status, which depicts the concentrated grids in and around Madhugiri taluk. The sensitive flora includes *Chloroxylon swietenia*, *Embelia tsjeriam-cottam*, *Santalum album*, *Aconitum heterophyllum*, *Saraca asoca*, *Shorea roxburghii*. Devarayanadurga, area

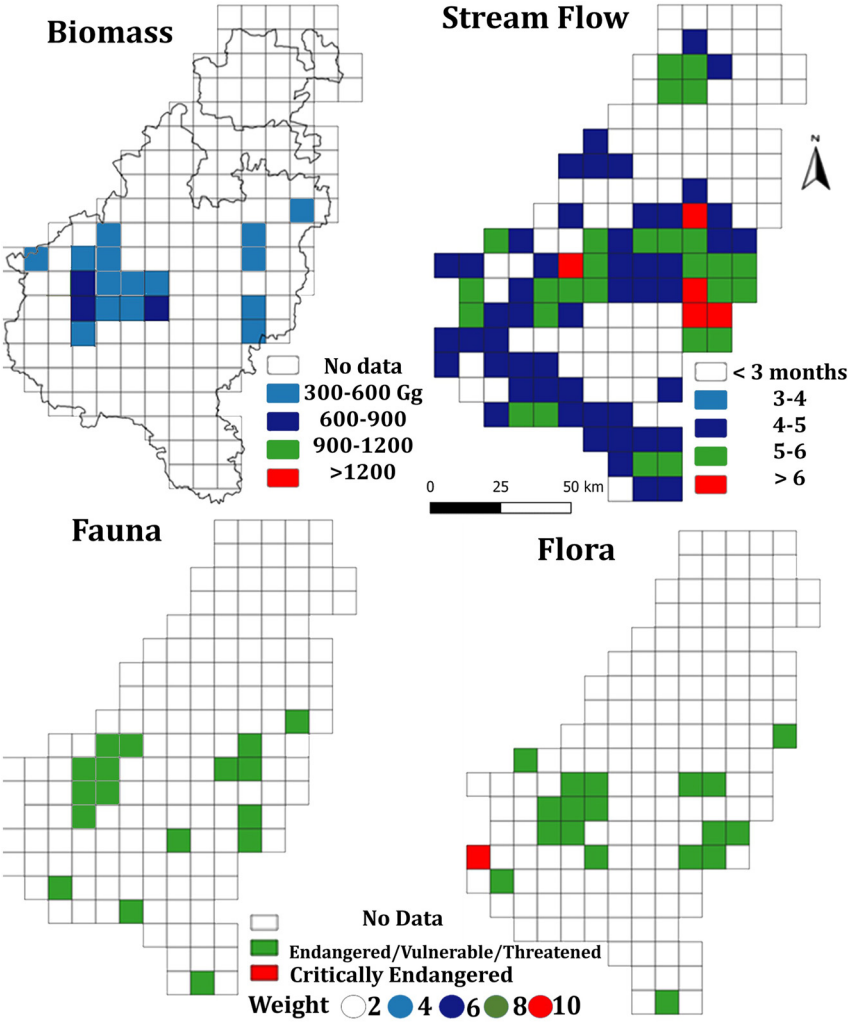

Figure 13: Ecological factors and their weights.

presents beautiful scenery of hill ranges with rich herbs intersected by agricultural valleys. Devarayanadurga region endowed with rich diversity of flora such as *Acacia leucophloea, Adina cardifolia, Albizia lebbek, Butea monosperma, Careya arborea, C. swietenia, Diospyros melanoxylon, Ficus glomerata, Gardenia latifolia, Mimosa pudica, Odina wodier, Phyllanthus emblica, Semecarpus anacardium, Thevetia nerrifolia, Tinospora cordifolia, Trema orientalis, Vicoa indica, Vittaria elongata, Wrightia tinctoria* [38]. The fauna species such as birds (*Ardeotis nigriceps, Gyps bengalensis, Gyps indicus, Sarcogyps calvus, Aquila nipalensis, Neophron percnopterus, Sterna acuticauda, Sypheotides indicus, Xantholaema malabarica, Anhinga melanogaster, A. melanogaster,*

Anthracoceros coronatus), mammals (*Antelope cervicarpa, Elephas maximus, Hyaena hyaena, Panthera pardus, Prionailurus rubiginosus, Melursus ursinus*) are considered as sensitive fauna of the district. The district is home to diverse reptiles such as Cobra, Indian Black Turtle, Russell's Viper, Bamboo Pit Viper, Bengal Monitor, Common Krait, Wolf Snake, etc. There is also a wide variety of butterflies, including crimson rose, mottled emigrant, lemon pansy, small orange tip, common rose, clipper, cruiser etc. Mydhannahalli Black Buck Conservation Reserve, Thimlapura Wildlife Sanctuary, Thimlapura Conservation Reserve and Bukkapatna Wildlife Sanctuary are protecting these sensitive species of flora and fauna.

Geo climatic variability has been assessed through a set of proxy variables, and weights were provided as depicted in Figure 14. Tumkur district has an annual rainfall of 743 mm with an average number of 46 rainy days. The taluks of Madhugiri, Koratagere, Sira and Turuvekre receive good rain as compared with others. The district has a slope of <15%, except for the regions covered with undulating hills with clumps of tall and well-grown trees. Elevation maps depict two major distinct classes.

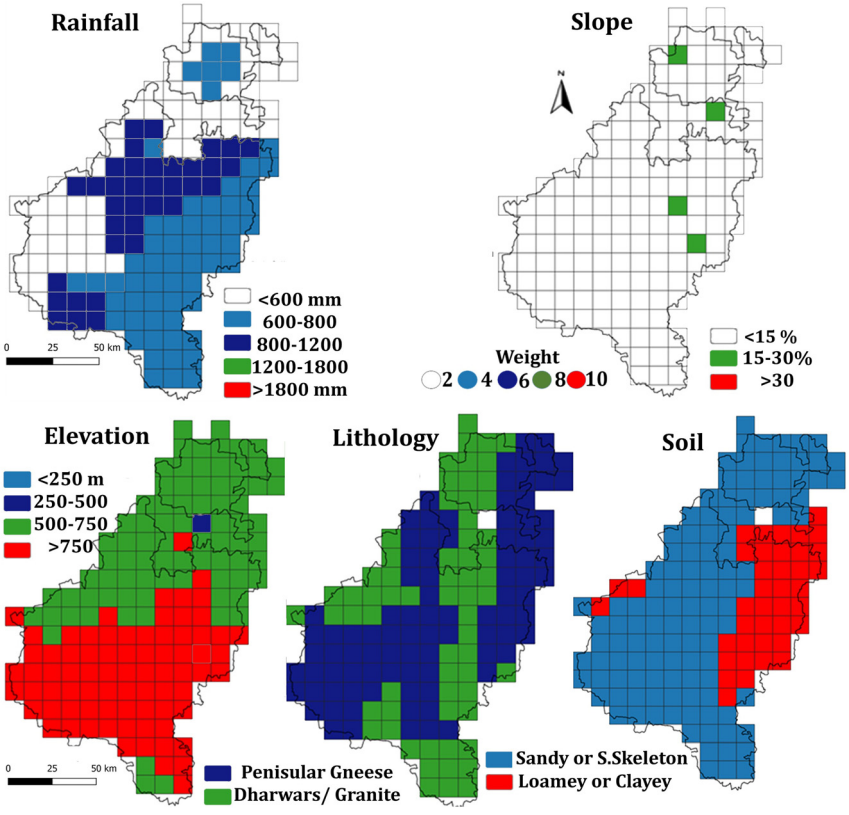

Figure 14: Geo-climatic factors assessed and their weights.

The Kunigal taluk consists mainly of undulating hills with plains interspersed. Long hill stretch running in the south–south east direction dominate the district's western part. The lithology of the district shows most of the region has gneese type followed by a thin variety of granitic hills categorized under closepet granites, which occupies the eastern part. These hills pass through the taluks of Madhugiri, Koratagere, Pavagada and northern parts of Tumkur. The district's soil (Sandy and clayey soil) shows as they are moderately eroded, shallow in depth and well-drained to excessively drained. The weights are assigned based on water infiltration and soil depth characteristics.

Population density (2011 census) information shows that the higher population density in Tumkur and other urban areas indicates 500–1000 persons per hectare (Figure 15). The higher weights were assigned for the regions of lower population density, as they signify less resource usage and least disturbances. The livestock density map shows Tiptur and Kunigal regions with the higher density of livestock (2.25–3), weights were assigned based on significance.

Aggregate weight for each grid was computed and grouped into four categories as ESR 1 (with aggregated values greater than mean + standard deviation), ESR 2 (values between mean + standard deviation and mean), ESR 3 (values between mean – standard deviation and mean), ESR 4 (values lower than mean – standard deviation). Figure 16 highlights that 1377 sq. km. in the district falls under ESR 1 (17 grids), 3726 sq. km falls under ESR 2 (46 grids), 5670 sq. km falls under ESR 3 (70 grids), and 1944 sq. km falls under ESR 4 (24 grids). The ESR 1 represents a zone of highest conservation, and no further degradation is allowed. ESR-2 has the potential to become ESR 1 provided with strict regulations and improvement of forests and their environs by more protection. A small change in ESR 2 will have more adverse effects on ESR 1. ESR 1 and ESR 2 – signifies

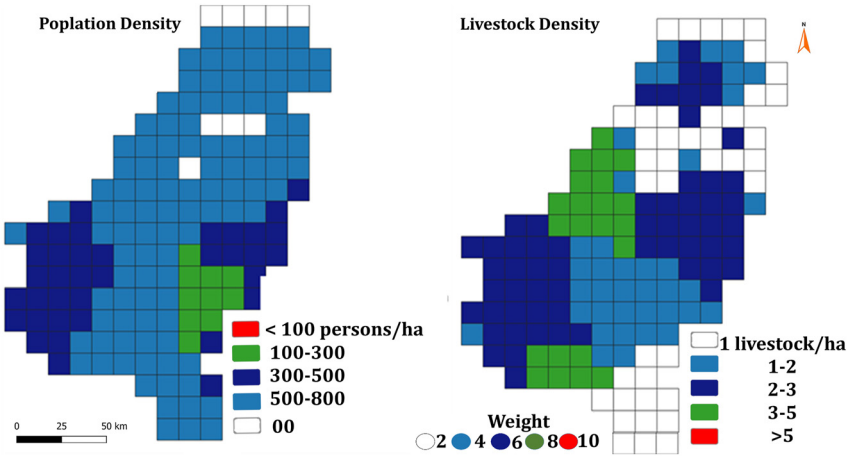

Figure 15: Population and interior forests of Tumkur and weight.

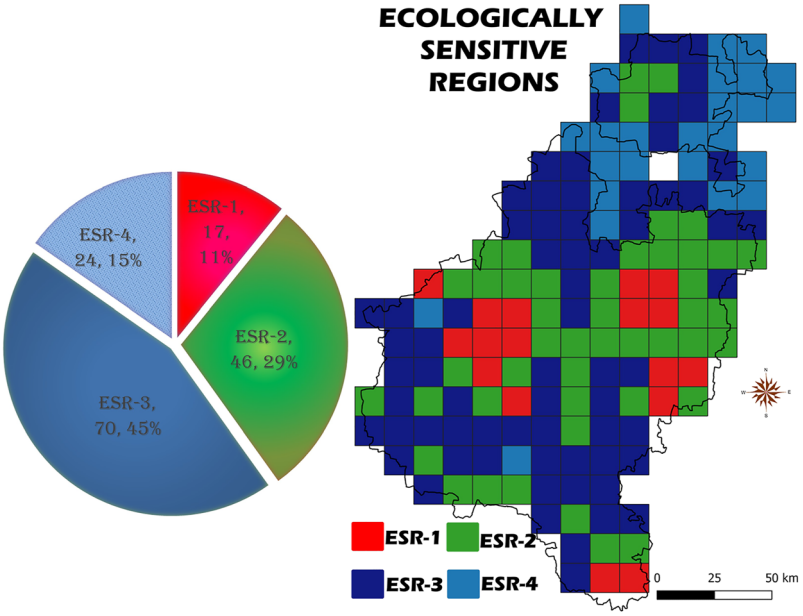

Figure 16: ESRs of Tumkur district.

that they are susceptible zones covered under the Madhugiri, Tiptur and Kunigal taluks, where absolutely no development activity such as dams and mining should not be allowed. ESR 3 is the region of sensitivity where agricultural and horticultural activity should be promoted, and large-scale industries should be restricted, but small-scale industries like IT sectors, and agro based can be encouraged. Tumkur district covers vast extent of coconut plantations under ESR 3 regions. ESR 4 is the region where large-scale industries and highly urbanized areas are present. Mainly city centers of the districts come under this category.

4 Conclusions

The comprehensive knowledge of temporal LULC changes and their impacts on ecological fragility is quintessential for evolving appropriate strategies for conservation. The increasing trend of built-up cover from 0.02 to 2.11% due to economic activities led to a decrease in agriculture and forest cover from 1989 to 2019. Fragmentation analysis further confirms this trend by depicting habitat loss and increased fragmentation at the regional scale. Modeling has aided in analyzing the trends of past LU changes and predicting the probability of future LU. The region might experience a likely increase of 5% built-up cover (2029) at the cost of agriculture and forest areas. Systematic

conservation by prioritization of ESR framework highlights 11% of the district under ESR 1, 29% under ESR 2, 15 45% under ESR 3, 4 respectively. The findings of likely LU change will help regional planners, and decision-makers control LULC changes, arrest habitat fragmentation, safeguard natural resources and frame common conservation strategies in the district.

Acknowledgments: We are grateful to the ENVIS division, the Ministry of Environment, Forests and Climate Change (MoEFCC), Government of India (GoI) for the sustained support to the ecological research in the Western Ghats. We acknowledge the infrastructure support by the Indian Institute of Science. We thank Karthik Naik for the assistance during the field data collection. We thank all the stakeholders for actively taking part in the scientific discussions and cooperation during field data compilation. We are grateful to the official languages section at IISc for the assistance in language editing.

Author contributions: All the authors have accepted responsibility for the entire content of this submitted manuscript and approved submission.

Research funding: This research was supported by the grant from ENVIS division, the Ministry of Environment Forests and Climate Change, Government of India.

Conflict of interest statement: The authors declare no conflicts of interest regarding this article.

Data and accessibility: Data used in the analyses are compiled from the field. Data is analyzed and organized in the form of tables, which are presented in the manuscript. Also, synthesized data are archived at http://wgbis.ces.iisc.ernet.in/energy/water/paper/researchpaper2.html#ce http://wgbis.ces.iisc.ernet.in/biodiversity/.

Research ethics: The publication is based on the original research and has not been submitted elsewhere for publication or web hosting.

Animal ethics: The research does not involve either humans, animals or tissues.

Permission to carry out fieldwork: Our research is commissioned by the Ministry of Environment, Forests and Climate Change (ENVIS Division), Government of India and hence no further permission is required as the field work was carried out in in the non-restricted areas/protected areas.

References

1. Twisa S, Buchroithner MF. Land-use and land-cover (LULC) change detection in Wami River Basin, Tanzania. Land 2019;8:136.
2. Bharath S, Rajan KS, Ramachandra TV. Land surface temperature responses to land use land cover dynamics. Geoinfor Geostat 2013;1:1–10.
3. Vinay S, Bharath S, Bharath HA, Ramachandra TV. Hydrologic model with landscape dynamics for drought monitoring. In: Proceeding of: joint international workshop of ISPRS WG VIII/1 and WG IV/4 on geospatial data for disaster and risk reduction, Hyderabad, November; 2013:67–72.

4. Ramachandra TV, Vinay S, Bharath S, Shashishankar A. Eco-hydrological footprint of a River Basin in Western Ghats. Yale J Biol Med 2018;91:431–44.
5. Tang X, Woodcock CE, Olofsson P, Hutyra LR. Spatiotemporal assessment of land use/land cover change and associated carbon emissions and uptake in the Mekong River Basin. Remote Sens Environ 2021;256:112336.
6. Birhane E, Ashfare H, Fenta AA, Hishe H, Gebremedhin MA, Solomon N, et al. Land use land cover changes along topographic gradients in Hugumburda national forest priority area, Northern Ethiopia. Remote Sens Appl 2019;13:61–8.
7. Tripathi OP, Upadhaya K, Tripathi RS, Pandey HN. Diversity, dominance and population structure of tree species along fragment-size gradient of a subtropical humid forest of Northeast India. Res J Environ Earth Sci 2010;2:97–105.
8. Ramachandra TV, Bharath S, Chandran MDS. Geospatial analysis of forest fragmentation in Uttara Kannada District, India. For Ecosyst 2016;23:10.
9. Galiatsatos N, Donoghue DNM, Watt P, Bholanath P, Pickering J, Hansen MC, et al. An assessment of global forest change datasets for national forest monitoring and reporting. Remote Sens 2020; 12:1790.
10. Laurance WF, Nascimento HEM, Laurance SG, Andrade A, Ewers RM, Harms KE, et al. Habitat fragmentation, variable edge effects, and the landscape-divergence hypothesis. PLoS One 2007;2: e1017.
11. Mengist W, Soromessa T. Assessment of forest ecosystem service research trends and methodological approaches at global level: a meta-analysis. Environ Syst Res 2019;8:22.
12. Reddy CS, Faseela VS, Unnikrishnan A, Jha CS. Earth observation data for assessing biodiversity conservation priorities in South Asia. Biodivers Conserv 2019;28:2197–219.
13. Bharath S, Ramachandra TV. An in-depth look at carbon emissions. In: Sreekanth KJ, editor. New York: Nova Science Publishers; 2021.
14. Uuemaa E, Antrop M, Roosaare J, Marja R, Mander Ü. Landscape metrics and indices: an overview of their use in landscape research. Living Rev Landscape Res 2009;3:1–28.
15. Kurnar D. Monitoring forest cover changes using remote sensing and GIS: a global prospective. Res J Environ Sci 2011;5:105.
16. Mairota P, Cafarelli B, Boccaccio L, Leronni V, Labadessa R, Kosmidou V, et al. Using landscape structure to develop quantitative baselines for protected area monitoring. Ecol Indic 2013;33: 82–95.
17. Bharath S, Ramachandra TV. Modeling landscape dynamics of policy interventions in Karnataka State, India. J Geovisual Spat Anal 2021;5:1–23.
18. Zeng C, He J, He Q, Mao Y, Yu B. Assessment of land use pattern and landscape ecological risk in the Chengdu-Chongqing economic circle, Southwestern China. Land 2022;11:659.
19. Ramachandra TV, Bharath S, Rajan KS, Chandran MDS. Modelling the forest transition in Central Western Ghats, India. Spat Inf Res 2017;25:117–30.
20. Harris NL, Goldman E, Gabris C, Nordling J, Minnemeyer S, Ansari S, et al. Using spatial statistics to identify emerging hot spots of forest loss. Environ Res Lett 2017;12:24012.
21. Rosa IMD, Purves D, Souza C Jr, Ewers RM. Predictive modelling of contagious deforestation in the Brazilian Amazon. PLoS One 2013;8:e77231.
22. Das P, Pandey V. Use of logistic regression in land-cover classification with moderate-resolution multispectral data. J Indian Soc Remote Sens 2019;47:1443–54.
23. Cai Z, Wang B, Cong C, Cvetkovic V. Spatial dynamic modelling for urban scenario planning: a case study of Nanjing, China. Environ Plan B Urban Anal City Sci 2020;47:1380–96.
24. Zhu W, Zhang J, Cui Y, Zhu L. Ecosystem carbon storage under different scenarios of land use change in Qihe catchment, China. J Geogr Sci 2020;30:1507–22.

25. Behera MD, Borate SN, Panda SN, Behera PR, Roy PS. Modelling and analyzing the watershed dynamics using Cellular Automata (CA)–Markov model–A geo-information based approach. J Earth Syst Sci 2012;121:1011–24.
26. Santé I, Garcia AM, Miranda D, Crecente R. Cellular automata models for the simulation of real-world urban processes: a review and analysis. Landscape Urban Plann 2010;96:108–22.
27. Bharath S, Rajan KS, Ramachandra TV. Status and future transition of rapid urbanizing landscape in central Western Ghats – CA based approach. ISPRS Ann Photogramm Remote Sens Spat Inf Sci 2014;8:69–75.
28. Zhang B, Xia C. The effects of sample size and sample prevalence on cellular automata simulation of urban growth. Int J Geogr Inf Sci 2022;36:158–87.
29. Wu Z, Ge Q, Dai E. Modeling the relative contributions of land use change and harvest to forest landscape change in the Taihe county, China. Sustainability 2017;9:708.
30. Das B, Pal SC. Assessment of groundwater vulnerability to over-exploitation using MCDA, AHP, fuzzy logic and novel ensemble models: a case study of Goghat-I and II blocks of West Bengal, India. Environ Earth Sci 2020;79:1–16.
31. Ramachandra TV, Bharath S, Chandran MDS, Joshi NV. Salient ecological sensitive regions of central Western Ghats, India. Earth Syst Environ 2018;2:15–34.
32. Aithal BH, Setturu B, Durgappa S, Ramachandra TV. Effectiveness of landscape spatial metrics with reference to the spatial resolution of remote sensing data. In: Proceedings of India conference on geo-spatial technologies & applications; 2012.
33. Riitters K, Wickham J, O'Neill R, Jones B, Smith E. Global-scale patterns of forest fragmentation. Conserv Ecol 2000;4:3.
34. Sang L, Zhang C, Yang J, Zhu D, Yun W. Simulation of land use spatial pattern of towns and villages based on CA–Markov model. Math Comput Model 2011;54:938–43.
35. dos Santos AR, da Silva Anjinho P, Neves GL, Barbosa MAGA, de Assis LC, Mauad FF. Dynamics of environmental conservation: evaluating the past for a sustainable future. Int J Appl Earth Obs Geoinf 2021;102:102452.
36. Bernasconi M, Choirat C, Seri R. The analytic hierarchy process and the theory of measurement. Manage Sci 2010;56:699–711.
37. Ramachandra TV, Setturu B, Vinay S, Tara NM, Subashchandran MD, Joshi NV. Geospatial infrastructure, applications and technologies: India case studies. In: Conservation and sustainable management of local hotspots of biodiversityGeospatial Infrastructure, Applications and Technologies: India Case Studies. Singapore: Springer; 2018:365–383 pp.
38. Bhat HR. A field guide to the Medicinal Plants of Devarayanadurga State Forest. Tumkur: Karnataka Forest Department; 2000, 37:1–168 pp.